Performance of an HRPPD in Tesla-scale magnetic fields

Author A[a,*], Author B[a,*], Author C[a]

[a] *Physics Department, Brookhaven National Laboratory, Upton, NY 11973, USA.*

Abstract

High Rate Picosecond Photodetectors (HRPPDs) are state of the art microchannel plate (MCP) photosensors with impressive single photon detection efficiency, position and timing resolution and are currently being considered for the ePIC experiment at the future Electron Ion Collider at Brookhaven National Laboratory. A necessary feature of this technology is reliable operation in a strong magnetic field up to 1.5 T, at an inclination of $\leq 15^o$ to the window surface normal. It has long been known magnetic field induced distortions of the collected charge in MCP-based detectors can be compensated by tuning the operating parameters, however, the objective of this study is to quantify this performance in the case of the EIC-HRPPD, a particular MCP stack-up specialized for operation within ePIC. This photosensor employs a high quantum efficiency photocathode, 10 μm capillary pores, thinner than typical transfer gaps, and a custom ceramic pixelated DC-coupled readout. This article explores the optimal operating parameters (mainly the voltage potentials applied across the gaps and MCPs) for single photon detection at various inclination angles in a uniform field up to 1.86 T. Ultimately, it was found that the gain and single photon detection efficiency of the HRRPD may be restored over a range of polar inclination angles up to $\pm 35^o$.

Keywords: Microchannel plate, HRPPD, LAPPD, RICH, ePIC, magentic field

1. Introduction

Modern micro-channel plate (MCP) photosensors offer distinct advantages that make them attractive options for radiation detection in high energy particle physics experiments. The High Rate Picosecond Photon Detector (HRPPD) is the latest generation MCP-based photosensor from Incom, Inc. [REF], based on its progenitor, the LAPPD [REF]. The HRPPD features a large aperture (10 cm $\times$ 10 cm active area) and a low profile (1.2 cm thick), up to 10^7 gain (enabling single photon detection), sub-millimeter position resolution, and a timing resolution approaching few tens of picoseconds or better. The photosensor package or "tile" incorporates a stack-up including a high quantum efficiency transmissive photocathode, followed by two microchannel plate (MCP) gain stages, and a charge collection anode (see Fig. 1). The ability to operate within a strong magnetic field, essential to many such experiments is also a key feature. In this article, we explore the performance of a sample HRPPD tile in a uniform static magnetic field, up to 1.86 T.

Though similar MCP-based detectors (including MCP-PMTs [REF] and LAPPDs [REF]) have already been shown to operate well in high magnetic fields [REF], we report on the particular characteristics of a so-called "EIC-HRPPD", designed for use in the ePIC experiment at the future Electron Ion Collider (EIC) at Brookhaven National Laboratory. The EIC-HRPPD was configured to operate in specified orientations in the ePIC magnetic field, with an inclination angle up to $\pm 15^o$ with respect to the window surface normal. The introduction of such a strong field complicates the flow of charge through the sensor stack, warranting a new study to both verify expected outcomes and to learn more about the detailed behavior of this stack up configuration.

As the magnetic field is intensified and the inclination angle increased, the transport of primary photoelectrons and subsequent avalanche electrons from the photocathode to the charge collection anode is increasingly modified. The trajectory of each electron is influenced by helical gyration, parallel acceleration, and $E \times B$ drift, resulting in non-negligible reductions in gain, broadening of the transit time spread, and a lateral displacement of the charge cloud with a reduced footprint on the anode plane. As each electron takes on a tighter helical-like motion, the incident angle at which it strikes the functionalized surface of the MCP capillary is effectively reduced, resulting in smaller energy transfer and a reduced probability for releasing secondary electrons. Furthermore, since the axis of the helical motion is aligned with the direction of the magnetic field, there exists the possibility to align the trajectory along the capillary axis, resulting in even fewer interactions with the capillary surface. Additionally, this helical motion has a focusing effect on the generation of the charge cloud by reducing the maximum electron recoil scattering angle off the various MCP surfaces, including the interstitial space between pores.

The EIC-HRPPD tile was customized to mitigate the source of such distortions and make the device less sensitive to strong magnetic fields. The design includes the reduction of the MCP pore diameter from 20 μm to 10 μm, which increases the chances of an electron interaction with the functionalized layer of the capillary to maintain the gain. Smaller pores also restrict

*Corresponding authors

Email addresses: email address A (Author A), email address B (Author B)

ion backflow, which helps to protect the photocathode from ion bombardment and extends its life. Also, by reducing the width of the transfer gaps, the EIC-HRPPD is less susceptible to magnetic deflection, beneficial to both lateral displacement and the transit time spread.

As such, HRPPD tiles are the baseline sensor modules for the ePIC pfRICH [REF], dRICH [REF], DIRC [REF], and TOF [REF] detector subsystems, and are candidates in other RICH applications, such as the Belle II ARICH at the Super KEKB accelerator [REF]. Since each detector system has unique and varied requirements for the photosensor, the goal of this study is to quantify the performance the EIC-HRPPD over a broad set of operating parameters, mainly the range of potentials applied across the MCPs and transfer gaps, as a function of the magnetic field strength and tile orientation. In doing so, we attempt to identify a stable operating point at each field value and inclination angle, characterized by adequate gain to provide sufficient photon detection efficiency (PDE), and optimal timing and position resolution.

2. Experimental Apparatus

2.1. HRPPD Sensor

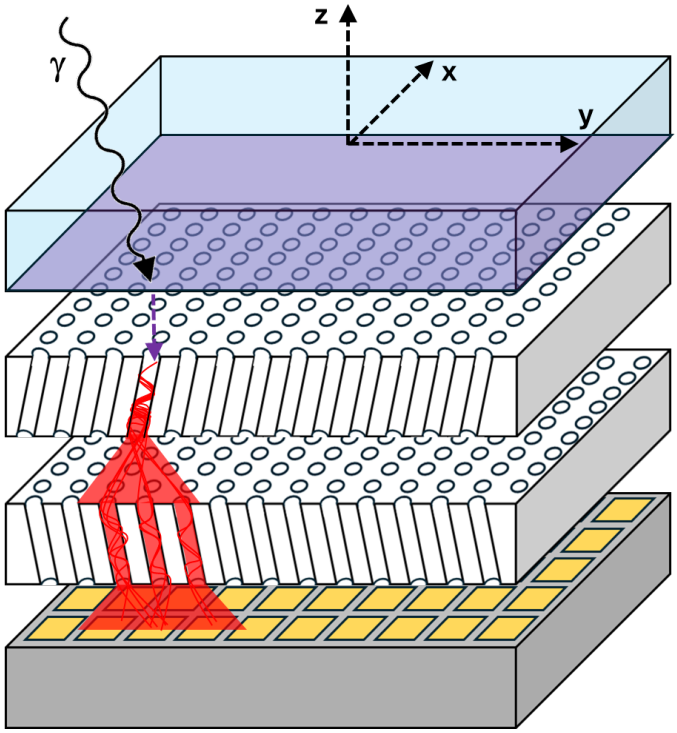

Figure 1: Sketch of HRPPD working principle (not to scale).

2.2. Detector Layout

2.3. DAQ and Slow Control

2.4. Test setup

3. Measurements and Results

3.1. Gain

3.1.1. Selection and Fitting

Explain the methodology for gain estimate here. Also show the spectra of integrated charge/gain, saturated and non-saturated ones.

3.1.2. Dependence on B-field Strength

Figure 2 demonstrates that the gain of the HRPPD decreases with stronger magnetic field. This falling trend is observed in a wide range of inclination angle. However, the gain can be recovered by setting a higher bias voltage on the MCPs. A bias voltage of about 675 V allows the HRRPD reaches a gain of 10^6 at a magnetic field of 1.5 T.

3.1.3. Dependence on Inclination Angle

Figure 3 shows the gain of the HRPPD as a function of the nominal inclination angles at various magnetic field. No inclination dependency is observe with the absence of a magnetic field. Consistent dips at $-12.5°$ and $15°$ are observed with the presence of a magnetic field. The previous angle refers to the alignment of the first MCP capillaries, while the latter refers the alignment of the second MCP capillary. These dips are observed when rotate with respect to either x or y axes. However, the dips are less pronounced in y-axis rotation. The reduction of gain when magnetic field is aligned to the MCP capillary indicates reduction of helical motion and subsequently the reduction of avalanche, as discussed in Section 1.

3.1.4. Dependence on High Voltage

Figure 4 shows that the gain of the HRPPD increases with higher MCP high voltage. The drops in gain at a inclination angle of $15°$, at voltage smaller than 680 V, and at magnetic field of 1.5 and 1.77 T are due to over subtraction of the pedestal.

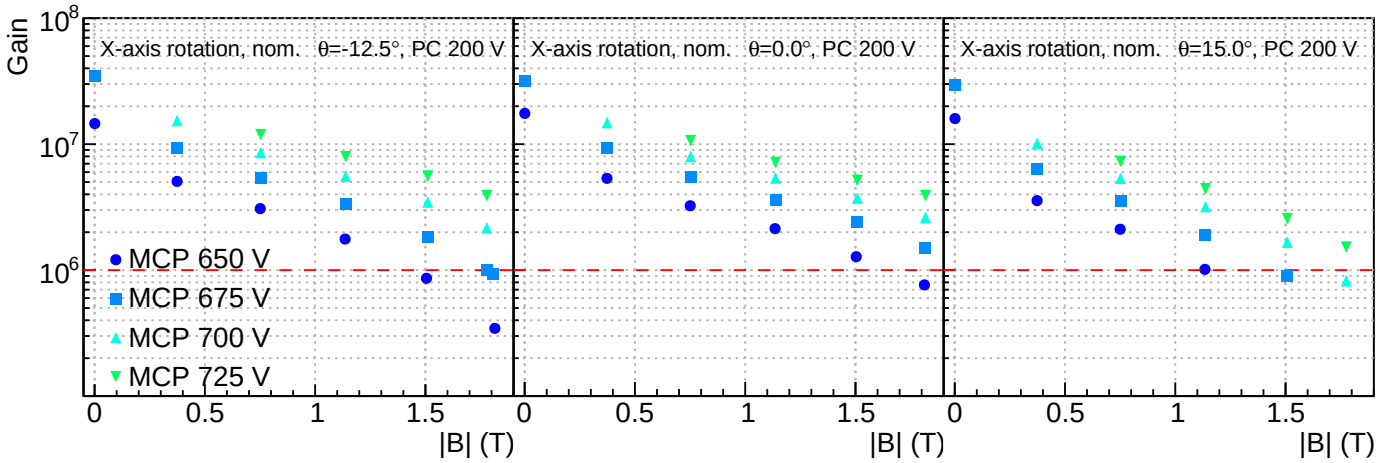

Figure 2: [PRELIMINARY] Gain as a function of magnetic field with a photocathode voltage of 200 V, and symmetric bias voltages on the MCPs. The red dashed line indicates a gain of 10^6.

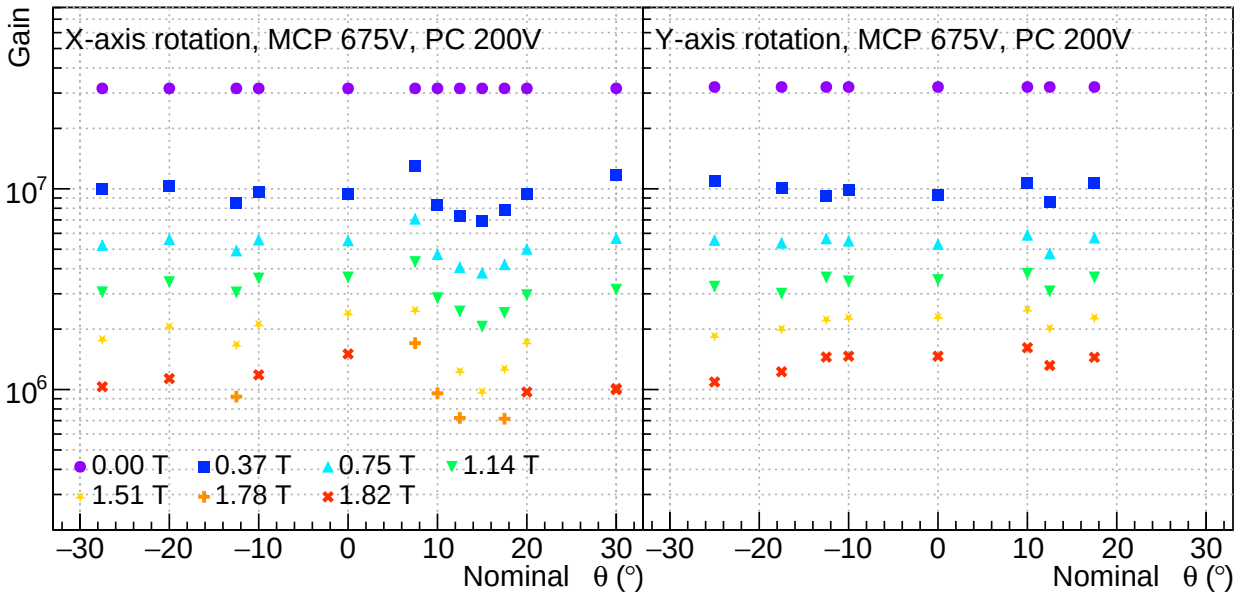

Figure 3: [PRELIMINARY] Gain as a function of inclination angle with a photocathode voltage of 200 V, and symmetric bias voltages of 675 V on the MCPs.

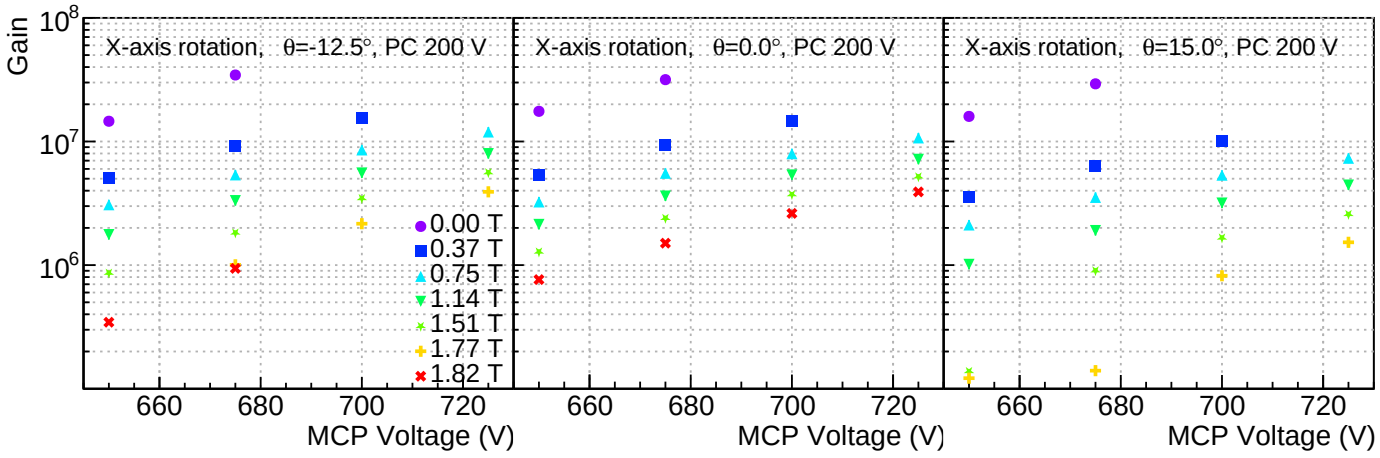

Figure 4: [PRELIMINARY] Gain as a function of high voltage with a photocathode voltage of 200 V.

3.2. Detection Efficiency

3.3. Afterpulsing rate

The afterpulsing rate was investigated using the peak-search algorithm within a 70 ns window following the primary signal peak. The amplitude threshold for afterpulse detection was set to be identical to that used for the primary signals. The HRPPD was placed within a uniform magnetic field of 1.3 T. At the nominal operating voltage of 675 V, the afterpulsing rate was measured at (1.34 ± 0.15)%. To identify the primary source of these pulses within the stack, the bias voltage of one MCP was increased in 25 V increments while the voltage on the other MCP was simultaneously decreased in 12 V steps to maintain a consistent order of magnitude for the gain. As illustrated in Figure 5, the afterpulsing rate exhibits a markedly higher sensitivity to the bias voltage of the first MCP compared to the second, indicating that the first MCP is the dominant contributor to afterpulsing.

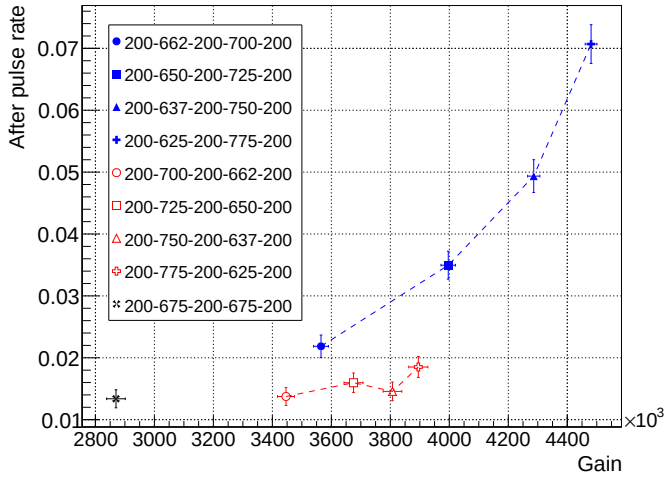

Figure 5: Measured afterpulsing rates across various HV configurations. The four data points connected by the blue dashed line represent HV settings where the first MCP is operated at a higher bias voltage relative to the second MCP.

To further isolate the origin of the afterpulses, the time separation between the primary signal peak and the subsequent afterpulse peak was calculated. As illustrated in Figure 6, a distinct peak occurs at approximately 6.4 ns (corresponding to 32 bins in the waveform recorded by the digitizer) when the first MCP is operated at a higher bias voltage. This timing interval is consistent with the flight time of H^+ ions originating from the bottom of the first MCP.

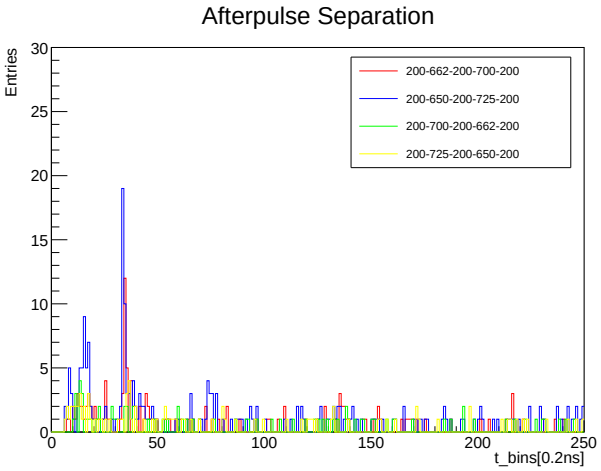

Figure 6: Time separation between the primary signal peak and the subsequent afterpulse peak for four HV settings near the nominal operating HV setting.

3.4. Dark count rate

To determine the dark count rate of the HRPPD, waveforms from 32 digitizer channels were analyzed with the laser switched off during data acquisition. The peak-search algorithm was used to identify dark-count events in these waveforms, with the signal amplitude threshold set at 4 mV. The resulting dark count rates, measured across a range of magnetic field strengths, are presented in Figure X.As a cross-check, a single pixel was connected to an oscilloscope using single-mode trigger. At a magnetic field strength of 1.8 T, the dark count rate was measured to be XX.

3.5. Time resolution

3.5.1. Results with Oscilloscope

3.5.2. Results with DSR4

The time interval between the midpoint of the trigger signal and the midpoint of the signal's rising edge was calculated, with the variance of this distribution serving as a measure of the timing resolution. To minimize electronic jitter, a time correction was applied to the DRS4 chips within the digitizer. Figure 7 illustrates the time separation for a representative dataset; the distribution is fitted with a Gaussian function, and the resulting σ is defined as the timing resolution. Note that the tail of the distribution, which corresponds to backscattered (bouncing) photoelectrons, has been truncated in the fitting range. The timing resolution was also measured across a range of magnetic field strengths, with the results summarized in Figure 8.

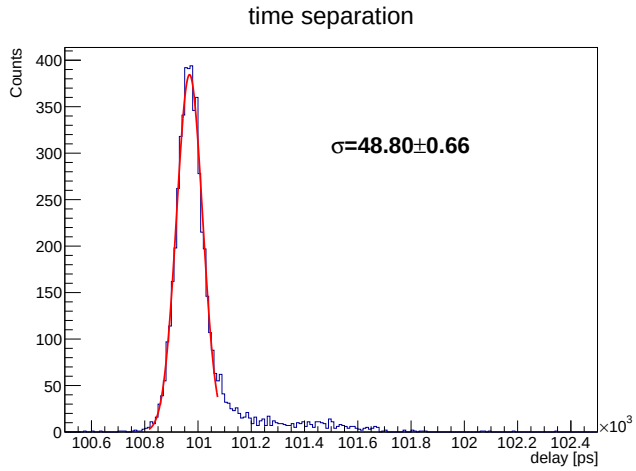

Figure 7: [PRELIMINARY] Time separation between the trigger and the signal of HRPPD.

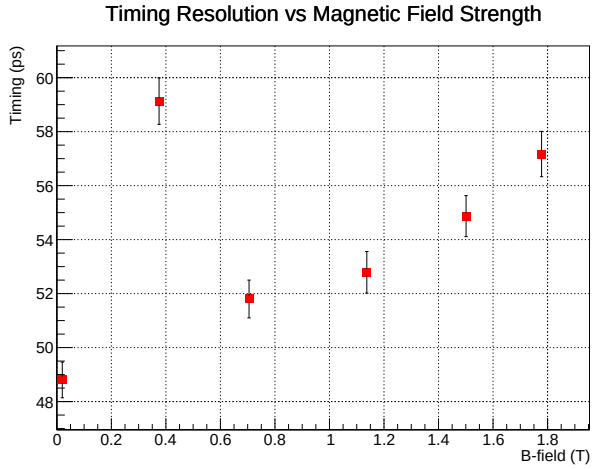

Figure 8: [PRELIMINARY] Timing resolution across a range of magnetic field strengths.

3.6. Position Resolution, maybe?

Since the beam spot is fixed, a simple histogram of the reconstructed beam spot position is a residual distribution by definition. Since the charge is shared among more than a single pad along both the X and Y axes, seems like we should be able to measure a centroid for both directions, no?

4. Discussions

4.1. Saturation due to signal rate

The aforementioned measurements were conducted at a trigger rate of 1.6 kHz. To investigate systematic effects arising from the dead time of the microchannels, a rate scan was performed. Here, the signal rate is defined as the product of the trigger rate and the fraction of events containing a valid signal. The measured gain as a function of signal rate is presented in Figure 9. The observed reduction in gain at higher signal rates indicates a saturation effect on the order of several percent. Consequently, in low-rate applications, a corresponding gain increase of a few percent is expected as the microchannels operate without charge depletion.

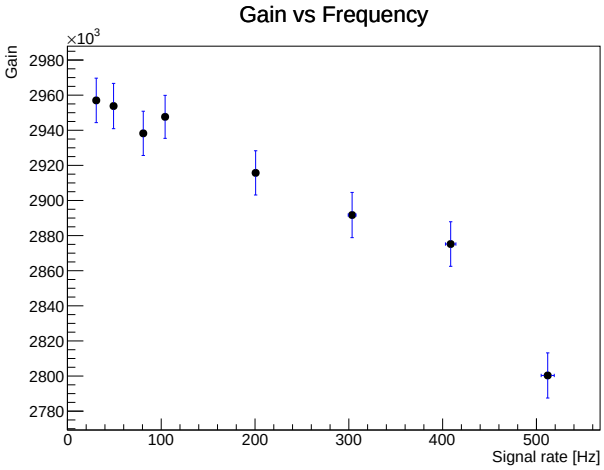

Figure 9: Gain with respect to signal rate. The third point from the left corresponds to a trigger rate of 1.6 kHz.

4.2. Tilting angles

4.3. Saturation of amplification in MCP#2

5. Conclusions

Acknowledgments

We are grateful to

References